Available online at www.sciencedirect.com
ScienceDirect
Journal of Power Sources 174 (2007) 544–547
JOURNAL OF POWER SOURCES
www.elsevier.com/locate/jpowsour

Short communication

Preparation and electrochemical properties of $Li[Ni_{1/3}Co_{1/3}Mn_{1-x/3}Zr_{x/3}]O_2$ cathode materials for Li-ion batteries

Bin Lin, Zhaoyin Wen *, Zhonghua Gu, Xiaoxiong Xu

Shanghai Institute of Ceramics, Chinese Academy of Sciences, Shanghai 200050, PR China

Available online 27 June 2007

Abstract

Layer-structured Zr doped $Li[Ni_{1/3}Co_{1/3}Mn_{1-x/3}Zr_{x/3}]O_2$ ($0 \le x \le 0.05$) were synthesized via slurry spray drying method. The powders were characterized by XRD, SEM and galvanostatic charge/discharge tests. The products remained single-phase within the range of $0 \le x \le 0.03$. The charge and discharge cycling of the cells showed that Zr doping enhanced cycle life compared to the bare one, while did not cause the reduction of the discharge capacity of $Li[Ni_{1/3}Co_{1/3}Mn_{1/3}]O_2$. The unchanged peak shape in the differential capacity versus voltage curve suggested that the Zr had the effect to stabilize the structure during cycling. More interestingly, the rate capability was greatly improved. The sample with $x = 0.01$ presented a capacity of 160.2 mAh g^{-1} at current density of 640 mA g^{-1}(4 C), corresponding to 92.4% of its capacity at 32 mA g^{-1}(0.2 C). The favorable performance of the doped sample could be attributed to its increased lattice parameter.

Keywords: Lithium ion battery; Cathode material; $Li[Ni_{1/3}Co_{1/3}Mn_{1/3}]O_2$; Zr-doping; Electrochemical performance

1. Introduction

In recent years, $Li[Ni_{1/3}Co_{1/3}Mn_{1/3}]O_2$ cathode material has been studied for use in Li-ion battery to replace the presently popular $LiCoO_2$ [1–7]. The predominant oxidation states of Ni, Co and Mn in this material are +2, +3 and +4, respectively. During delithiation, the Ni^{2+} ions are oxidized to Ni^{4+} while the oxidation state of Mn^{4+} remains unchanged [8]. This material has attracted significant interests because the combination of nickel, manganese and cobalt could provide many advantages such as higher reversible capacity with milder thermal stability at charged state, lower cost and less toxicity than $LiCoO_2$. Thus, $Li[Ni_{1/3}Co_{1/3}Mn_{1/3}]O_2$ might be one of the most promising cathode materials for high-energy, high-power lithium-ion batteries [2].

Despite the positive effect of $Li[Ni_{1/3}Co_{1/3}Mn_{1/3}]O_2$ for the electrochemical property, the delivered capacities have shown a fading during long-term cycling [3]. Therefore, the addition of dopants or the surface modification of $Li[Ni_{1/3}Co_{1/3}Mn_{1/3}]O_2$ has been studied to prevent fading of the discharge capacity. For example, $Al(OH)_3$ has been coated on $Li[Ni_{1/3}Co_{1/3}Mn_{1/3}]O_2$ powder to improve cycling performance [9], but it lowers the discharged capacity compared with the bare $Li[Ni_{1/3}Co_{1/3}Mn_{1/3}]O_2$. Several authors suggested that anionic substitution for oxygen appears to be a good method to modify the structure and electrochemical properties of $Li[Ni_{1/3}Co_{1/3}Mn_{1/3}]O_2$ [10–12]. Moreover, the developing history of cathode materials proved that partial substitution for transition metal was an effective method in modifying the electronic structure and improving the electrochemical performances.

In this paper, Zr doped $Li[Ni_{1/3}Co_{1/3}Mn_{1/3}]O_2$ was prepared by slurry spray drying method. The Zr dopant was selected because of its bigger size than that of Mn^{4+} ions and stronger Zr–O bond. Moreover, as Mn^{4+} is electrochemically inactive during cycling, the substitution of tetravalent Zr^{4+} for Mn^{4+} would not sacrifice the discharge capacity. The effects of Zr doping on structure and electrochemical properties were investigated.

2. Experimental

2.1. Sample preparation

The stoichiometric amounts of precursors Li_2CO_3, NiO, Co_3O_4, $MnCO_3$ and ZrO_2 (10% excess Li was used to compensate possible Li loss during the calcination and sintering process) were mixed in alcohol solvent by rotary ball milling

* Corresponding author. Tel.: +86 21 52411704; fax: +86 21 52413903.
E-mail address: zywen@mail.sic.ac.cn (Z. Wen).

0378-7753/$ – see front matter © 2007 Elsevier B.V. All rights reserved.
doi:10.1016/j.jpowsour.2007.06.125

with zirconia balls as milling bodies at a speed of 300 rpm for 2 h to form a slurry, then 6 wt.% polyvinyl butyral (PVB) was added and dissolved in the slurry and mixed for another 1 h. Then, the slurry was spray-dried with a spray-drier (Niro 2108. Copenhagen, Denmark). The dried spherical powders were heated at 1000 °C for 10 h in an alumina crucible.

2.2. Characterization

Scanning electron microscope (SEM, JEOL JSM-6700F) was applied to observe the morphology and particle size of the synthesized materials. Powder X-ray diffraction (XRD, Rigaku RINT-2000) measurement using Cu Kα radiation was employed to identify the crystalline phase of the synthesized materials. The scan range was 5°–80° with a scan step of 0.02° and a scan speed of 10° per min. The chemical composition of the synthesized materials was determined by an inductively coupled plasma spectrometer (ICP, IRIS Advantage 1000).

The electrochemical performance of the powders was evaluated with coin-type cells (CR 2025) with a lithium foil counter electrode and an electrolyte consisting of a 1 M $LiPF_6$ solution in EC:DMC (1:1, v/v) at room temperature. Microporous polypropylene membrane (Celgard) was used as the separator. The working electrode was prepared from a paste of 80 wt.% of the active powders with 10 wt.% conductive acetylene black and 10 wt.% PVDF binder in NMP solvent. The paste was then coated on an aluminum foil, and finally dried under vacuum at 100 °C for 10 h before electrochemical evaluation. The battery was assembled in a glove box (VAC AM-2) filled with pure argon. All the cells were allowed to age for 10 h before testing. The galvanostatic charge–discharge tests were conducted on a LANDCT2001A battery test system with the cut-off voltages of 2.5 and 4.5 V (versus Li/Li^+).

3. Results and discussion

The morphology of the synthesized powders was observed using SEM. It was showed that the morphology of the spheres of the powder was no obviously changed as the Zr was doped. The typical image of $Li[Ni_{1/3}Co_{1/3}Mn_{1-x/3}Zr_{x/3}]O_2$ ($x = 0.01$) was shown in Fig. 1. The precursors were spherical and uniform with size of about 40 μm. After calcining, the spherical particles shrank and pores were formed after the decomposition of PVB binder. Detailed observation of the $Li[Ni_{1/3}Co_{1/3}Mn_{1-x/3}Zr_{x/3}]O_2$ ($x = 0.01$) powder showed that the particle was composed of micron sized primary particles.

ICP analysis results revealed that the chemical composition of final $Li[Ni_{1/3}Co_{1/3}Mn_{1/3}]O_2$ after heating at 1000 °C for 10 h was $L_{i1.01}Ni_{0.329}Co_{0.336}Mn_{0.335}O_2$, which implied the zirconia milling bodies had little contamination of as-prepared samples during ball milling. Fig. 2 showed the XRD patterns of $Li[Ni_{1/3}Co_{1/3}Mn_{1-x/3}Zr_{x/3}]O_2$ ($x = 0$, 0.01, 0.03 and 0.05) samples. The XRD peaks were narrow, indicating high crystallinity of the products. All of peaks could be indexed based on the α-$NaFeO_2$ structure, and no impurity phase was observed in the range of $0 \le x \le 0.03$. However, some low intensity bands in the 22°–23° angular regions appeared while the amount of Zr

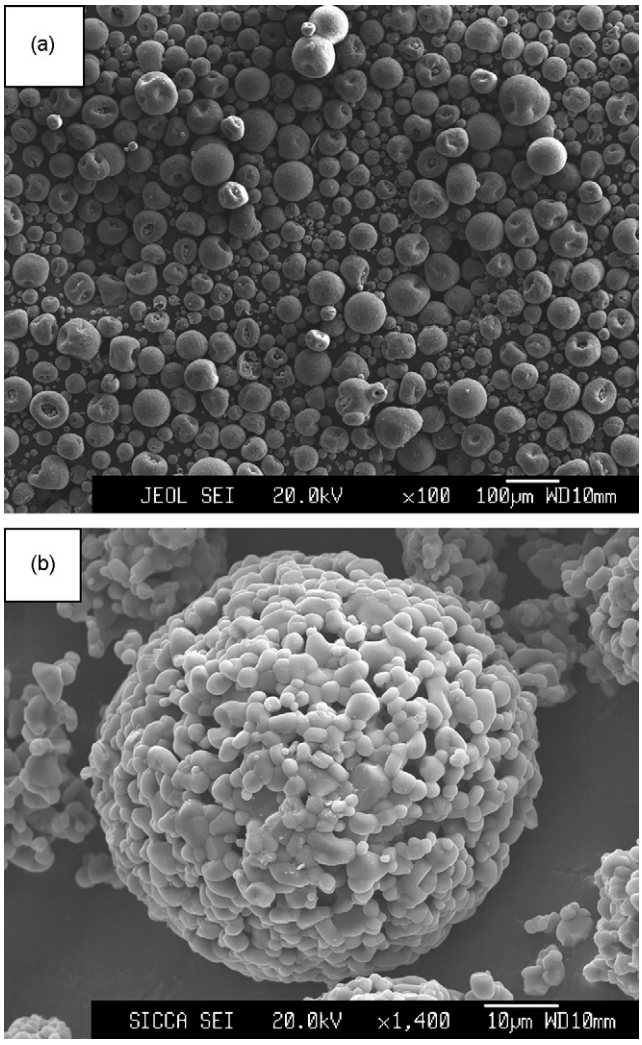

Fig. 1. SEM of (a) precursor of $Li[Ni_{1/3}Co_{1/3}Mn_{1-x/3}Zr_{x/3}]O_2$ ($x = 0.01$) by spray drying method and (b) $Li[Ni_{1/3}Co_{1/3}Mn_{1-x/3}Zr_{x/3}]O_2$ ($x = 0.01$) calcined at 1000 °C.

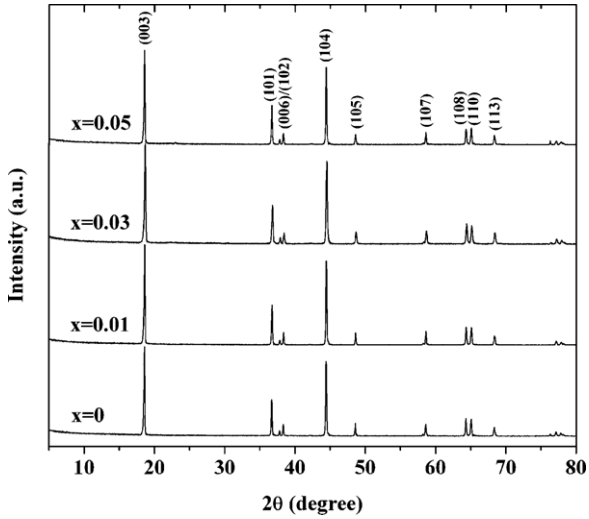

Fig. 2. XRD patterns of $Li[Ni_{1/3}Co_{1/3}Mn_{1-x/3}Zr_{x/3}]O_2$ ($x = 0$, 0.01, 0.03 and 0.05).

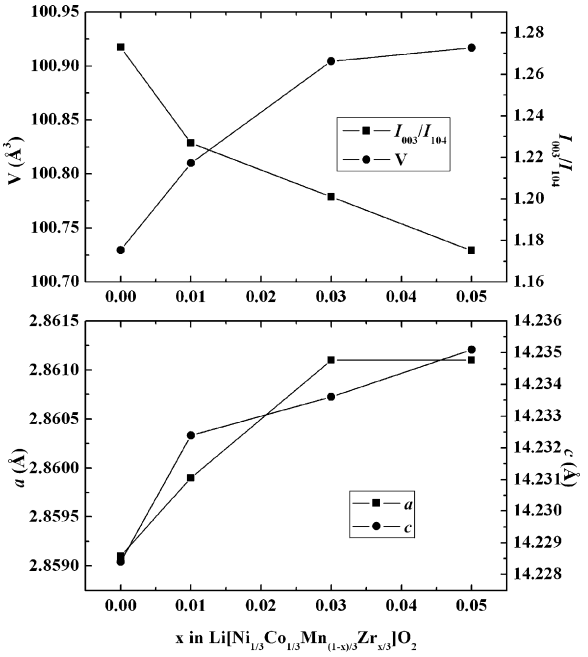

Fig. 3. Variation of lattice parameters as a function of Zr amount in $Li[Ni_{1/3}Co_{1/3}Mn_{1-x/3}Zr_{x/3}]O_2$.

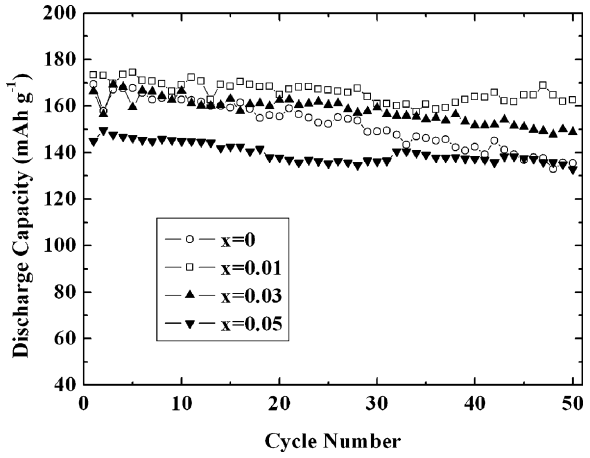

Fig. 4. Cycling performance of Li/$Li[Ni_{1/3}Co_{1/3}Mn_{1-x/3}Zr_{x/3}]O_2$ cells cycled between 2.5 and 4.5 V.

increased to 0.05, which would be attributed to the superlattice ordering of the Li, Ni, Co and Mn in the 3a site (transition metal layer), indicating a layered structure with the Li_2MnO_3 character [13,14].

Fig. 3 demonstrated the dependence of lattice parameters *a* and *c* on *x* of $Li[Ni_{1/3}Co_{1/3}Mn_{1-x/3}Zr_{x/3}]O_2$. The lattice parameters were calculated by a least square method based on the XRD patterns of Fig. 2. It could be found that both the *a* and *c* values of the compounds increased with increasing Zr content, leading to the increased volume of the unit cell. This was attributed to the bigger radius of the Zr^{4+} in comparison with the Mn^{4+}. According to [15], the effective ionic radii of Mn^{4+} and Zr^{4+} were 0.645 and 0.72 Å, respectively. So it was reasonable that substitution of Zr^{4+} for Mn^{4+} in $Li[Ni_{1/3}Co_{1/3}Mn_{1/3}]O_2$ lead to lattice expansion in both the *a* and *c* directions.

Fig. 4 was a plot of the specific discharge capacity versus the cycle number for $Li[Ni_{1/3}Co_{1/3}Mn_{1-x/3}Zr_{x/3}]O_2$ ($x = 0$, 0.01, 0.03 and 0.05) at a constant current density of 32 mA g^{-1} (0.2 C rate) at room temperature. The initial discharge capacity of the un-doped sample was about 169.5 mAh g^{-1}. Compared with the un-doped one, doped samples with $x = 0.01, 0.03$ exhibited comparable discharge capacity, i.e., 173.4 and 169.2 mAh g^{-1}, respectively. The reversible capacity of $Li[Ni_{1/3}Co_{1/3}Mn_{1-x/3}Zr_{x/3}]O_2$ was due to $Ni^{2+/4+}$ and $Co^{3+/4+}$ redox pairs. Because the electrochemically active amount of Ni^{2+} and Co^{3+} remained the same as those of $Li[Ni_{1/3}Co_{1/3}Mn_{1/3}]O_2$, the zirconium substitution for Mn sites did not cause obvious capacity changes. However, the sample of $x = 0.05$ had a discharge capacity of only 149.6 mAh g^{-1}. As discussed previously, the lower capacity might be related to the low-intensity bands in the 22°–23° angular regions in the XRD of $x = 0.05$. After 50th cycling, the average fading rate per cycle for un-doped $Li[Ni_{1/3}Co_{1/3}Mn_{1/3}]O_2$ and Zr-doped $Li[Ni_{1/3}Co_{1/3}Mn_{1-x/3}Zr_{x/3}]O_2$ ($x = 0.01$) were 0.40% and 0.12%, respectively. From the electrochemical properties summarized in Table 1, it was obvious that the cycling performance of Zr-doped material was better than that of pure one.

Fig. 5 showed differential capacity versus voltage of the 5th, 15th, 25th and 35th cycles for the $Li[Ni_{1/3}Co_{1/3}Mn_{1-x/3}Zr_{x/3}]O_2$ ($x = 0.01$). From the un-changed redox peak, it could be seen that structural change did not occur during the repetitive lithium extraction/insertion processes. Therefore, Zr doping of $Li[Ni_{1/3}Co_{1/3}Mn_{1/3}]O_2$ was an effective means to substantially enhance cycling performance.

Rate capability test also demonstrated the advantages of Zr substitution. Fig. 6 showed the dependence of discharge capacity of $Li[Ni_{1/3}Co_{1/3}Mn_{1-x/3}Zr_{x/3}]O_2$ on the applied current densities. The cells were charged at 32 mA g^{-1} (0.2 C) and discharged at 32, 80, 160, 320 and 640 mA g^{-1}. The discharge capacity of the un-doped sample dropped dramatically with increasing current densities, from 169.5 mAh g^{-1} at current density of 32 mA g^{-1} to 120.5 mAh g^{-1} at 640 mA g^{-1},

Table 1
Electrochemical properties of $Li[Ni_{1/3}Co_{1/3}Mn_{1-x/3}Zr_{x/3}]O_2$ ($x = 0$, 0.01, 0.03 and 0.05)

Sample	Initial discharge capacity (mAh g^{-1})	Fading rate per cycle (%)	Rate capability (ratio of discharge capacity (%))				
			0.2 C	0.5 C	1 C	2 C	4 C
$x = 0$	169.5	0.40	100	90.1	84.0	77.5	71.1
$x = 0.01$	173.4	0.12	100	99.4	97.2	94.8	92.4
$x = 0.03$	166.3	0.21	100	99.2	97.5	95.2	91.0
$x = 0.05$	144.9	0.22	100	99.5	98.1	93.9	89.7

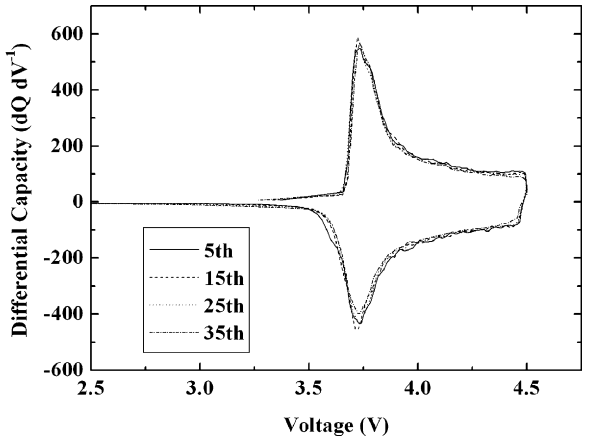

Fig. 5. Differential capacity vs. voltage for $Li[Ni_{1/3}Co_{1/3}Mn_{1-x/3}Zr_{x/3}]O_2$ ($x = 0.01$).

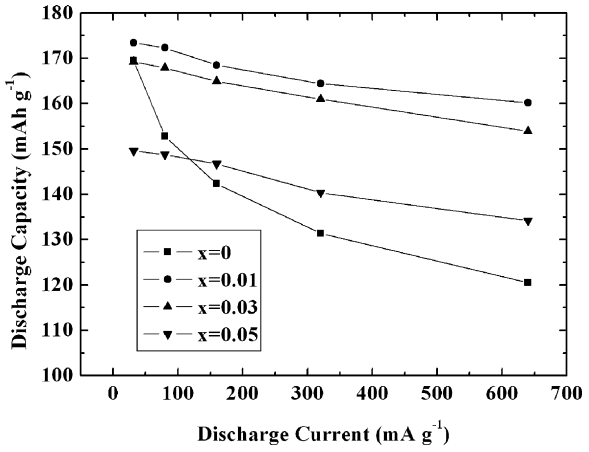

Fig. 6. Rate capability of $Li/Li[Ni_{1/3}Co_{1/3}Mn_{1-x/3}Zr_{x/3}]O_2$.

respectively. However, the rate capability was improved significantly by Zr doping. The sample $Li[Ni_{1/3}Co_{1/3}Mn_{1-x/3}Zr_{x/3}]O_2$ ($x = 0.01$) presented a capacity of 160.2 mAh g^{-1} at current density of 640 mA g^{-1}, corresponding to 92.4% of its capacity at 32 mA g^{-1}, showing the best rate capability among all the samples. In brief, Zr doping was favorable to improve the rate capability of $Li[Ni_{1/3}Co_{1/3}Mn_{1/3}]O_2$. This was related to larger lattice parameter caused by Zr doping, which could enable Li ion to move more freely in the oxide.

4. Conclusions

Zr doped $Li[Ni_{1/3}Co_{1/3}Mn_{1-x/3}Zr_{x/3}]O_2$ ($0 \le x \le 0.05$) was prepared and characterized. The products remained single-phase within the range of $0 \le x \le 0.03$. It was demonstrated that the Zr substitution for Mn site in $Li[Ni_{1/3}Co_{1/3}Mn_{1/3}]O_2$ provided enhanced cycle life and rate capability to the un-doped one, while did not cause the reduction of the discharge capacity. The unchanged peak shape in the differential capacity versus voltage curve suggested that the Zr had the effect of stabilize the structure during cycling. Moreover, the $Li[Ni_{1/3}Co_{1/3}Mn_{1-x/3}Zr_{x/3}]O_2$ ($x = 0.01$) had the best rate capability among all the presented samples, presenting a capacity of 160.2 mAh g^{-1} at current density of 640 mA g^{-1}, corresponding to 92.4% of its capacity at 32 mA g^{-1}, which could be attributed to the increased lattice parameter by Zr-doping.

Acknowledgment

This work was financially supported by key project of Natural Science Foundation of China (NSFC) No. 20333040.

References

[1] T. Ohzuku, Y. Makimura, Chem. Lett. (2001) 642.
[2] I. Belharouak, Y.K. Sun, J. Liu, K. Amine, J. Power Sources 123 (2003) 247.
[3] K.M. Shaju, G.V. Subba Rao, B.V.R. Chowdari, Electrochim. Acta 48 (2002) 145.
[4] N. Yabuuchi, T. Ohzuku, J. Power Sources 119–121 (2003) 171.
[5] H. Yoshizawa, T. Ohzuku, Electrochemistry 71 (2003) 1177.
[6] Z.X. Wang, Y.C. Sun, L.Q. Chen, X.J. Huang, J. Electrochem. Soc. 151 (2004) A914.
[7] N. Yabuuchi, T. Ohzuku, J. Power Sources 146 (2005) 636.
[8] W.S. Yoon, C.P. Grey, M. Balasubramanian, X.Q. Yang, D.A. Fischer, J. McBreen, Electrochem. Solid-Sate Lett. 7 (2004) A53.
[9] S.B. Jang, S.H. Kang, K. Amine, Y.C. Bae, Y.K. Sun, Electrochim. Acta 50 (2005) 4168.
[10] G.H. Kim, S.T. Myung, H.J. Bang, J. Prakash, Y.K. Sun, Electrochem. Solid-Sate Lett. 7 (2004) A477.
[11] S.T. Myung, G.H. Kim, Y.K. Sun, Chem. Lett. 33 (2004) 1388.
[12] G.H. Kim, S.T. Myung, H.S. Kim, Y.K. Sun, Electrochim. Acta 51 (2006) 2447.
[13] J.S. Kim, C.S. Johnson, J.T. Vaughey, M.M. Thackeray, Chem. Mater. 16 (2004) 1996.
[14] Y.K. Sun, C.S. Yoon, Y.S. Lee, Electrochim. Acta 48 (2003) 2589.
[15] R.D. Shannon, Acta Cryst. A32 (1976) 751.